FERЯE User's Guide

C. Allende Prieto

July 7, 2022

FERRE is an analysis code written in FORTRAN90. It matches models to data, identifying the model parameters that best reproduce observations. Model predictions are to be given as an array whose values are a function of the model parameters, i.e. numerically. FERRE holds this array in memory, or in a direct-access binary file, and interpolates in it. The code returns, in addition to the set of parameters, their error covariance, and the corresponding model prediction.

Contents

1   Introduction

Using models to interpret observations is a very common task in science. Models may be sophisticated, sometimes the result of solving complex sets equations, and can only be evaluated numerically in some cases. The data sets to be analyzed may be large, regarding both the number of objects and the data per object. And so can be the models, which may involve a large number of parameters.

FERRE matches physical models to observed data. It was created to deal with the common problem of having numerical models that are costly to evaluate, and need to be used to interpret large data sets. FERRE provides flexibility to search for all model parameters, or only some them holding constant the others. The code is written to be truly N-dimensional and fast. The merit function to evaluate agreement between models m_i and observations o_i (with uncertainties $\sigma_i(o)$) is the χ^2 square

$$\chi^2 = \sum_i \frac{1}{\sigma_i^2(o)}(m_i - o_i)^2. \tag{1}$$

Models are to be encapsulated in a multi-dimensional array, with as many dimensions as parameters. The model array is held in memory for speed, but it can also be written in disk ans used as a data base. Models are interpolated with a choice of algorithms (linear, Bezier quadratic, cubic, and cubic splines), with interpolations carried out in a sequential fashion.

Several optimization algorithms are available to search for the best-fitting model parameters: the Nelder-Mead algorithm (Nelder & Mead 1965), the Boender-Timmer-Rinnoy Kan global algorithm (Boender et al. 1982), Powell's UOBYQA algorithm (Powell 2000), a Truncated Newton algorithm (Dembo & Steihaug 1983), or a weighted sum over the parameters space. Several schemes are also available for estimating error bars on the derived abundances.

Some applications can benefit from data compression applied to models based on Principal Component Analysis, and parallelization over multiple cores, which are both handled in a way that is fairly transparent to users. FERRE has a history of successful applications to the analysis of astronomical spectra since 2003 (see §10).

2   Optaining and compiling the code

FERRE is free software. It is written in FORTRAN90, and parallelized with OpenMP. It is been successfully compiled with gfortran, g95, the Intel compiler (ifort), the Sun Studio Compiler, the PGI compiler, the IBM compiler (xlf90), and a few other.

The code can be obtained from
`https://github.com/callendeprieto/ferre`

You should end up with four folders: src (the 'code'), test (test data), bin (empty folder for the executables), and doc (this manual). Change directories to src and invoke make to compile the code
>cd ferre/src
>make
and you should end up with two executables, one for FERRE ('a.out', copied to the bin folder as 'ferre.x') and another one (ascii2bin) for converting model grids from text format to (direct-access) binaries.

3   Running the code

To run FERRE we need a model grid (see Section 4), a control file (`input.nml`; see §5), and input data files (see §6.1). Once all these are in place, we simply need to invoke the ferre executable from a working directory, where the aforementioned files (or symbolic links to them) need to be. After describing the format for the input files, we illustrate how to run FERRE with examples in Section 7.

4   Model grid

In order to run FERRE you need to make your model predictions available as a data file. The model of your choice will predict the same quantities that we have observations for, as a function of the model parameters. This is precisely what is in the file that contains the model grid, a multi-dimensional array with as many dimensions as model parameters. In general, there will be multiple observations, e.g. multiple quantities or the same quantity observed as a function of time. This gives one additional dimension to the model grid. The grid must be perfectly regular, i.e. if two parameters are considered, and the first one is sampled with 4 values and the second one with 6 values, the grid will have 24 models, corresponding to all possible combinations of the values for the two parameters.

   The format of the file that contains the model grid (a.k.a. the SYNTH module) is very simple. Each model prediction, corresponding to a given combination of parameters, takes a full line in the file. In our previous example with two parameters, and 4 and 6 values for each of the parameters, respectively, the file would have 24 lines. If the array of observed quantities has 20 elements, then each line in the file will have 20 columns. The numbers (model predictions) are preceded by a header explaining the contents. The order of the model predictions can be easily recovered. Since the grid is regular, a series of nested loops, according to the information specified in the file header, gives the values of the parameters that correspond to each line in the file.

   An example may help. If we are dealing with spectroscopy of stars, and the observations are relative photon fluxes at different wavelengths, our model grid could include spectra predicted as a function of effective temperature, surface gravity, and metallicity[1]. If we consider a model grid of spectra that includes 100 wavelengths, with 10 effective temperatures, 10 gravities, and 10 metallicities, our grid file will have 1000 lines, with 100 columns each.

   Since the model grids are perfectly regular, with constant steps in the parameters that define them, a few quantities can describe them. Those quantities are provided in the header of the file. For example, the values that correspond to each of the parameters can be described with a linear equation, $Y = aX + b$, one for each parameter. The relevant coefficients are given in the file header, identified with the keywords LLIMITS (coefficient b) and STEPS (coefficient a).

   The model grid file always begins with the line

`&SYNTH`

which tells FERRE the header is a name list with that name. Only a few of the keywords possible in the grid header are mandatory:

- n_of_dim: Number of dimensions (parameters) of the model grid,

- n_p: An array with the number of data points in the grid for each dimension (it is an array with as many elements as dimensions the grid has),

---

[1]Most stars are approximately made of 80% H, 18% He, and about 2% of the rest of elements. It is the latter group of elements, those heavier than He, what matters the most for shaping stellar spectra, and as such it is one of the parameters that needs to be considered in models.

Table 1: Parameters that can be used in the header of a FERRE model grid. Only the first few at the top of the list are usually required.

Parameter	Type (elements)	Meaning
Mandatory	Parameters	
n_of_dim	integer	Number of dimensions
n_p	integer (n_of_dim)	Number of data points per dimensions
npix	integer	Number of observations per sample
llimits	integer (n_of_dim)	Lower limits for the model parameter arrays
steps	integer (n_of_dim)	Steps for each of the parameter arrays
Optional	Parameters	
multi	integer	Number of headers after the main one
synthfile_internal	string	Internal name of the model grid file
id	string	File identifier
date	string	Date when the file was assembled
npca	integer (*)	Number of PCA components per PCA section
label	string (n_of_dim)	Tags identifying the parameters of the model
transposed	integer	A value > 0 indicates data are transposed
comments1...6	Comment fields	
Optional	Parameters	intended for use with spectroscopic data
wave	float (2)	Coeffs. in $\lambda = \mathrm{wave}(1) + (i\text{-}1)*\mathrm{wave}(2)$ (i=1...npix)
logw	integer	Values of 0/1/2 indicate we use $\lambda/\log10(\lambda)/\ln(\lambda)$
vacuum	integer	Values of 0/1 indicate air/vacuum wavelengths
resolution	float	Resolving power (λ/FWHM) of the spectra
original_sampling	float	Velocity sampling in original calculations (km/s)
synspec	integer	When > 0 indicates spectra computed with Synspec
modo	integer	When synspec=1, this the value of 'imode'
invalid_code	float	Value used to indicate data are unavailable
constant	float	Constant value subtracted to the entire grid
continuum	float (4)	Coefficients used for continuum normalization
precontinuum	float (4)	Coefficients for a pre-normalization
file_data19	string	Atomic line list used in the synthesis
file_data20	string	Molecular line list used in the synthesis

- npix: Number of data points per sample (frequencies for spectroscopy),

- llimits: Array with the minimum values for each of the model parameters, and

- steps: Array with the steps (difference between two consecutive nodes) for each dimension.

These, and other optional keywords are listed in Table 1. Many of the optional keywords are intended to deal with spectroscopic data; they are mainly for tracking the contents of the file, and they are clearly marked in Table 1.

5 Control file

The control file is named `input.nml`. It tells FERRE what to do: the dimensions of the problem, the name of the input files, how to search for the solutions, or how to interpolate. The control files must always begin with the line

```
&LISTA
```
As with the model grid file, only a few of the keywords are mandatory:

- ndim: Number of dimensions/parameters the problem has (must match n_of_dim in the model grid file),

- nov: Number of parameters to vary (those we wish to search for; the remainder of the parameters will be held at constant values of the user's choice),

- indv: Array of indices corresponding to the parameters to vary (following the order given in the model grid),

- synthfile(1): File name for the model grid (can use several),

- pfile: Parameter file (name of the file with 'input' parameters; see §6.1 for details),

- ffile: Data file (name of the file with the observations; see §6.1 for details),

- erfile: Error data file (name of the file with the uncertainties associated to the data file, in the same format; see §6.1 for details),

- opfile: Output parameter file (output from FERRE, which contains the best-fitting model parameters for each sample), and

- offile: Output data file (output from FERRE, containing the best-fitting model predictions for each sample).

These and the remainder of the possible keywords are explained in Table 2.

6 Input/output parameter and data files

Usually FERRE will take, in addition to the model grid and the control file, three input files, and produce two output files. We describe below the contents and format for these files.

6.1 Input data files

- Input parameter file (`pfile`; usually associated with the .ipf file extension): This file contains an identifier for each spectrum in the first column, and then as many additional columns as parameters in the model grid (ndim). The values for the parameters do not need to be known unless we are holding some of them constant in the search. By default, the searches are initialized at the values in the center of the grid, but one can also choose to start at the values given in the input parameter file, or at other locations (see §8.3).

- Input flux file (`ffile`, usually associated with the .frd extension): This file contains the actual spectra to be fit. Each line is a spectrum, with as many columns as frequencies (npix). In many applications the spectrum will be sampled exactly on the same frequencies as the model grid, but if the two do not match the code can interpolate (see §8.5).

- Input Error file (`erfile`; OPTIONAL, .err): This file has exactly the same format as the input flux file, but with the uncertainties in the fluxes instead of the fluxes themselves. If the signal-to-noise ratio is constant, this file can be omitted and the keyword SNR can be used instead in the control file (input.nml).

- Input wavelength file (`wfile`; OPTIONAL, .wav): This file specifies the wavelengths associated with each input spectrum when these do not match those in the model grid.

Table 2: Parameters that can be used in the FERRE control file (`input.nml`). Only the first few at the top of the list are mandatory (default values in parenthesis).

Parameter	Type (elements)	Meaning
Mandatory	Parameters	
ndim	integer	Number of dimensions/parameters (should match n_of_dim)
nov	integer	Number of parameters to search
		nov=0 if we just want to interpolate in the grid
indv	integer (nov)	Array with the indices for the parameters to search
synthfile	string (*)	File name(s) for the model grid(s)
pfile	string	Name of the input parameter file
ffile	string	Name of the input data file (the observations we want to model)
erfile	string	Name of the file with the uncertainties in the input data
opfile	string	Name of the output parameter file with the optmized parameters
offile	string	Name of the output best-fitting models
Optional	Parameters	
nobj	integer	Number of samples (spectra) to analyze (all by default)
nlambda	integer	Number of data points (frequencies) per sample
f_format	integer	Format of the model grid (0 for text or 1 for binary)
f_access	integer	Mode of accessing the model grid data
		0 for RAM or 1 for direct-access
inter	integer	Interpolation algorithm (default 1)
		0 for nearest neighbor
		1 for linear
		2 for quadratic Bézier
		3 for cubic Bézier
		4 for cubic splines
errbar	integer	Choice of algorithm to compute error bars (default 0)
		0 to adopt the distance from the solution at which
		$\chi^2 = \min(\chi^2) + 1$
		1 to invert the curvature matrix
nruns	integer	Number of searches to be done (default 1)
init	integer	Choice of starting point(s) for searches (default 1)
		0 to use the values in `pfile`
		1 to follow the rules set by keyword indini
indini	integer (ndim)	Individual control of starting points for each param. (default 1)
		-1 start at the value in `pfile`
		0 start at random
		1 start at the grid center
		>1 start at the center of indini(i) equidistant cells
		[requires setting nruns $= \prod_i \text{indini}(i)$]
wfile	string	Name of the input data file with wavelengths
		[same format as ffile or erfile]
lsffile	string	Name of the input data file with information on the LSF
winter	integer	Switch to wavelength interpolation (default 0)
		0 No interpolation
		1 Interpolate observations, 2 fluxes (both require wfile)
algor	integer	Search algorithm (default 1)
		1/2/3/4 for Nelder-Mead, Boender-Timmer-Rinnoy Kan,
		Powell's or Nash's truncated Newton algorithms
lsf	integer	LSF shape (0/1/2/3/4/11/12/13/14 – default is 0)
nthreads	integer	Number of threads for parallel processing (default 1)

6.2 Output data files

FERRE will usually produce two output files

- Output parameter file (`opfile`; usually with an extension .opf): with a format similar to the input parameter file, plus additional columns. The first column is identical to the first one in the .ipf: the identifier for each spectrum. This is followed by as many columns as parameters in the grid (ndim), with the values fixed or derived in the search. Up to this point the .opf is identical to the .ipf in format, but then there is again ndim additional columns with the uncertainties in the parameters (these will be zero for the parameters that were held constant). Three more columns follow, giving the fraction of photometric data points (useful when multiple grids combining spectroscopy and photometry are used), the average $\log(S/N)^2$ for the spectrum, and the logarithm of the reduced χ^2 for the fit. Additional columns with the covariance matrix of the errors can be output setting to 1 the keyword COVPRINT. Since the matrix is symmetric, only the elements on the diagonal and above are printed (row by row), a total of ndim$\times$(ndim+1)/2 elements.

- Output flux file (`offile`; .mdl): With the same format as the input flux file, this file contains the best-fitting model, derived by interpolation in the grid for the corresponding parameters in the output parameter file.

7 Examples

Bundled together with the source code, there are several examples, all based on a grid of models made for the blue arm of the DESI spectrographs (Abareshi et al. 2022). The grid is in the file `n_rdesi2-b.dat`, which is a 3D grid of model stellar spectra spanning the range $3579 \leq \lambda \leq 5958$ Å, that covers $-5 \leq$ [Fe/H] ≤ 0.5, $5500 \leq T_{\text{eff}} \leq 8000$ K, and $1 \leq \log g \leq 5$. We will first interpolate models in the grid, then analyze a set of fake observations to inferred the model parameters, and lastly fix two of the parameters and derive the third.

7.1 interpolating in a grid

The control file, described in Section 5, has a keyword `nov` to specify how many of the `ndim` dimensions in the grid are to be searched. The same keyword, set to zero, can be used to interpolate spectra.

As an exercise we will interpolate three models in the aforementioned stellar grid. We will get spectra for a star like the Sun ([Fe/H]= 0, $T_{\text{eff}} = 5777$ K, and $\log g = 4.437$), and two more similar stars, but with lower metallicity, [Fe/H]= -1 and -2.

The control file has to be named `input.nml`, so we will copy the example in `input.nml_interpol` to `input.nml`. This file looks like this

&LISTA
NDIM = 3
NOV = 0
SYNTHFILE(1) = 'n_rdesi2-b.dat'
PFILE = 'interpol.ipf '
OFFILE = 'interpol.mdl'
/

Only the minimum necessary parameters are included in this file: we state the number of dimensions, tt nov=0 for interpolation, the grid name, an input parameter file with the desired parameters, and an output flux file where the interpolated fluxes will end up.

To run the code in the test directory, where the input parameter file and the input.nml file are, call the ferre executable

> ../src/a.out

and watch the standard output information come out. Go ahead, plot the data in `interpol.mdl` (one spectrum per line, each with 4759 columns/wavelengths) and examine how the depth of the lines reduces with the metal abundance of the star. If you want to reconstruct the wavelength scale of the spectra, look at the information in the WAVE and NPIX keywords in the header of the model grid: $\lambda = 0.5 \times (k-1) + 3579.19995117$, with $k = 1, 2..., 4759$. By default the interpolation is linear in all the parameters, but this can be changed as explained below.

7.2   inferring all the parameters in the grid

Next we will try to fit a bunch of fake observations. The observations must have the same resolution as the model grid (coded in the RESOLUTION keyword in the header of the grid), and be sampled on the same wavelength scale for consistency. In this case or *observations* are nothing but models from the grid to which we have injected Gaussian noise at a 10% level.

This example is given in the file `input.nml_all`, which looks like this

```
&LISTA
NDIM = 3
NOV = 3
INDV= 1 2 3
SYNTHFILE(1) = 'n_rdesi2-b.dat'
PFILE = 'rdesi2-b.ipf '
FFILE = 'rdesi2-b.frd '
ERFILE = 'rdesi2-b.err'
OPFILE = 'rdesi2-b.opf'
OFFILE = 'rdesi2-b.mdl'
SFFILE = 'rdesi2-b.nrd'
CONT = 1
NCONT = 0
ERRBAR = 1 /
```

Again, this is a nearly minimal file that specifies the number of dimensions `ndim`, how many we're actually searching `nov`, their indices `indv`, the name of the grid file, the input parameters, observations and error bars (`pfile, ffile, erfile`), as well as the name for the sought-after parameters (`opfile`) and best-fitting spectra (`offile`). Since tt cont is equal 1 we are normalizing the observations and the models on the fly with a polynomial. The parameter `ncont` is set to 0, so we are normalizing by a constant – dividing the observed spectra and the interpolated models by their respective mean values. With the keyword `sffile` we indicate the output file for the normalized data – the normalized version of the input data in `ffile`. We also have an optional keyword for telling FERRE how to compute the error bars. By default the code uses a simple procedure that looks how far one has to perturb the solution to cause a large change in the χ^2 (`errbar=0`), but setting `errbar=1` makes the code to invert the curvature matrix and take the diagonal for the variances.

As in the previous example, we copy the file `input.nml_all` to `input.nml` and run ferre in the test directory

../src/a.out

where the output files will appear after a few seconds. Plot one of the spectra in the input file `rdesi2-b.frd` – there is one per line. The file `rdesi-bnrd` contains the normalized version of these data, which is what FERRE is fitting. You will find these are identical to the input data but scaled to have a mean value of unity. Compare one of the normalized spectra
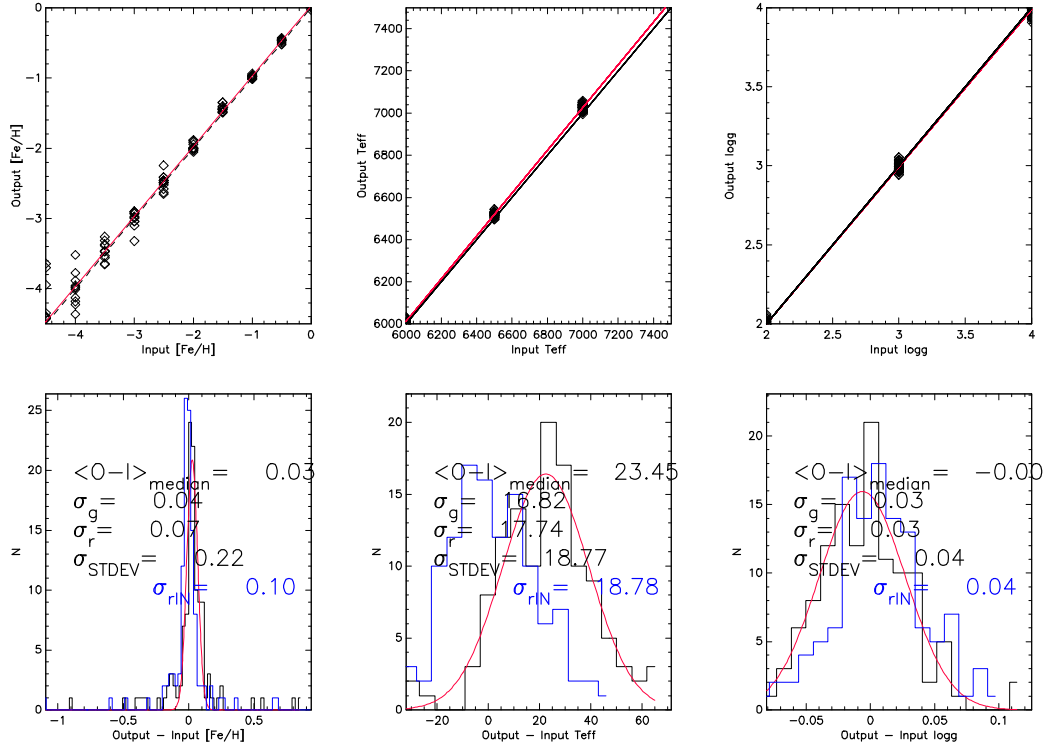
Figure 1: Comparison between the parameters for the simulated *observations* and those recovered by FERRE: parameters 1, 2 and 3 correspond to [Fe/H], T_{eff}, and $\log g$, respectively. The top panel shows the output (recovered) parameters versus the input ('true') values, and the bottom panels show (black histograms) the distribution of residuals (recovered – true). The red curves are Gaussian fitted to the data. The blue histograms show the distribution of uncertainties estimated by the code (`errbar=1`). In addition to estimates of the mean offset and distribution width from the Gaussian fits (<O–I> and σ_g), the lower panels show a robust determination (σ_r) and a straight calculation of the standard deviation (σ_s).

with the best fitting model in the same row of the `rdesi2-b.mdl` file. Look at the best-fitting parameters in `rdesi2-b.opf` and compare them with the true parameters of the fake observations in `rdesi2-b.ipf`. In some cases, especially at low metallicities, the errors are significant. Fig. 1 shows some statics for the residuals of the spectra in this example.

In this case, since we are fitting all three parameters, the input parameter file does not need to include sensible starting values. By default the code starts searching at the grid center, but there are several other options available (see §8.3).

7.3 holding constant some parameters while fitting others

Ferre gives you flexibility about what parameters to search and which ones to hold constant. If we repeat the previous exercise but change in `input.nml`
NOV = 1
INDV = 2
the search will only be done for the second parameter of the grid (T_{eff}), holding constant the first and the third ([Fe/H] and $\log g$) to the values in the input parameter file (`rdesi2-b.ipf`), which is our test case contains the 'true' values for the simulated *observations*.

8 Advanced use

The following sections are devoted to described some of the features of FERRE that go beyond the most basic use.

8.1 Multiple ways of storing and accessing the model grid

One of the keys for speed in FERRE is holding the model grid on which models are interpolated in the RAM memory of the computer. One pays the penalty of having to read the entire grid in memory before starting the optimizations, but then the merit-function evaluations proceed much faster than having to read the models from a hard drive. For large grids, reading the data from disk can still be painful. This can be reduced significantly by storing the grid in binary form.

FERRE comes with a tool for transforming from text to binary any properly formatted grid: ascii2bin. For example, to transform to binary format the grid in the test directory type
../src/ascii2bin
and the code will ask for the input file ('n_rdesi2-b.dat' in this case).

Once the code is finished, you should end up with two new files: `n_rdesi2-b.hdr`, which contains the header, and `n_rdesi2-b.unf`, which holds the unformatted (binary) data. Once you have the model grid converted, you can start using it this fashion immediately by adding the keyword
F_FORMAT=1
to your `input.nml`. If you are pressed for space, at this point you can remove or compress the ascii (.dat) version of the model grid, replacing its name on the `input.nml` file by the smaller file containing only the header (.hdr).

Sometimes the model grid may be too large to keep in the RAM. Or we may be in the situation that the time to load it in memory exceeds the actual optimization time, perhaps because we only have one or a few objects to fit. In that case we can avoid loading the grid in memory, accessing the models as they are needed directly from the hard drive. To do this, we just need to switch on another keyword in the `input.nml`
F_ACCESS=1
This requires that the model grid has been previously converted to binary format as desbed above, so that the 'records' in it are perfectly structured (and therefore `F_FORMAT=1` in your `input.nml`).

8.2 High order interpolation

By default the interpolations in the model grid (the 'library') are linear. This means the keyword INTER=1. Higher order interpolation can be used, and are generally recommended for accuracy by changing INTER to 2 (Bézier quadratic), 3 (Bézier cubic), or 4 (cubic splines). Mészaros & Allende Prieto (2013) have performed a systematic study of the uncertainties associated with the multidimenaional interpolation of stellar spectra.

8.3 Initialization of the searches

By default FERRE performs only one search for the best solution. However, sometimes is usefult to perform several searches per object, helping to make sure we don't get stuck in a local minimum. NRUNS sets the number of searches, while INIT and INDINI set where each should start. By default NRUNS, INIT and INDINI are set to 1, and therefore there is only one

search starting at the center of the grid. Setting INIT to 0 will change the behavior of the code to start the searches at the values in `pfile`.

When NRUNS is set to an integer larger than 1 and INIT is set to 1 the code will start each of the NRUNS searches at a different location chosen at random values of the parameters. This can be changed to start at specific locations by setting INDINI to an array of values, each corresponding to the number of initializations in a given dimension. For example, if we are working with a three-dimensional problem and want to perform 8 searches evenly distributed over the parameter space, we should set NRUNS=8, and INDINI= 2 2 2. Similarly, perform 4 searches for each input object starting at points equidistant from the center in the first and third dimension, but at the central value of the grid for the second parameter we would set instead INDINI= 2 1 2.

8.4   Excluding data from the fittings

We may be in the situation that we have missing data for some objects (e.g. a piece of the spectrum affected by severe distortions), or simply that our data span a wider wavelength range than our model grid. In those cases we can avoid including the missing regions in the χ^2 evaluation by setting the input fluxes to zero, or similarly, make their contribution to the χ^2 negligible by inflating the uncertainties for those data points.

8.5   Smoothing and interpolating models on the fly

FERRE, by default, expects the wavelengths of the model grid (those at which the model fluxes have been sampled) and the observations to match. If they don't, we can set the keyword WINTER to 1 or 2, and perform linear interpolations on-the-fly. For this keyword to work, we need of course to know the wavelengths of the data in the input flux file `ffile` (see Table 2; those for the model grid are coded in its header). Needless to say, it is of course preferred to interpolation the noiseless models (WINTER=2) than the data.

If our spectral line spread function (LSF) depends on wavelength, time, slit position, etc. the best solution is to have a model grid with a resolutiison higher than that of the data, performing a smoothing with the right LSF on the fly. This can be achieved by setting LSF to the right value, passing the appropriate information through `lsffile`. The choices are as follows:

- 0 – no LSF convolution (default)

- 1 – 1D (independent of wavelength), one and the same for all spectra

- 2 – 2D (a function of wavelength), one and the same for all

- 3 – 1D and Gaussian (i.e. described by a single parameter, its width), one for all objects

- 4 – 2D and Gaussian, one for all objects

- 11 – 1D and particular for each spectrum

- 12 – 2D and particular for each spectrum

- 13 – 1D Gaussian, but particular for each spectrum

- 14 – 2D Gaussian and particular for each object.

The format of the `lsffile` depends on the LSF case. Of course there is no such file for LSF=0. When the LSF is Gaussian, the same for all wavelengths (1D), and the same for all targets (LSF=3), then only the width of the Gaussian is needed, i.e. the `lsffile` will only contain a single number: the FWHM of the Gaussian in units of pixels of the library. When it is Gaussian, 1D, and depends on the target, the LSF file should have a single number per line. When it is 2D (wavelength dependent) and Gaussian, but common to all targets, the LSF file should contain a single line, with as many columns as wavelengths in the grid (NPIX), giving the FWHM values.

The most complex cases are when the LSF is not Gaussian, but it is specified numerically, as an array. When it is 1D and common for all targets, the LSF file should have a single line with the actual LSF, sampled on the same pixel step as the library. When it is 2D and common to all targets, the LSF file should give a 2D array with as many columns as wavelengths in the library, and with the LSF for each wavelength given in each column. Finally, when it is 2D and particular for each target the LSF file should contain a series of 2D arrays with the same format just described for each object, one after another. For example, if the LSF is described numerically as an array of 10 pixels and depends on wavelength for a library with NPIX=120 wavelengths, the LSF for a series of 3 targets will contain 3 2D arrays in a row, each written to the file with 120 columns and 10 lines. Such a file will have 120 columns and 30 lines.

The sampling in wavelength/velocity space for the LSF must be exactly the same as the library's. Smoothing and interpolation can be used in combination.

8.6 Continuum normalization

Continuum normalization is a common procedure in the analysis of high-resolution stellar spectra. Usually the relative flux levels over small wavelength intervals are measured with far greater precision that the absolute flux or even the relative flux variation over longer wavelength ranges. Continuum normalization consists in removing low frequency variations, retaining the fast ones corresponding to the sharp aborption/emission features corresponding to atomic or molecular transitions.

Traditionally low-order polynomials are iteratively fitted to the data. Sigma-clipping or similar algorithms are used to reject the absorption/emission lines, so that the polynomials track the variations in the continuum. Then data are divided by the polynomials to remove the slow continuum variations. This is the algorithm implemented in IRAF[2], which is usually applied interactively.

Performing continuum normalization within FERRE ensures that **exactly the same** code is run on both models and data. Consistency is highly desirable in this step in order to achieve the best possible results. The iterative sigma-clipping algorithm described above involves a non-linear transformation, and therefore the result depends on the signal-to-noise of the data, and therefore iterations are not implemented and only one pass is performed in FERRE. Setting CONT=1 in the control file activates the polynomial fitting. The keyword NCONT must then be set to the order desired for the polynomial (0 for a constant, 1 for a straight line, etc.). One can optionally exclude data points with relative errors larger than a threshold (REJECTCONT), using a parameter with the same name.

Two additional algorithms for continuum normalization are available:

- Segmented normalization (CONT=2): the input data arrays are split into NCONT segments, and the values in each are divided by their mean values (see Fig. 1 and associated

---

[2]IRAF, the Image Reduction and Analysis Facility, is a general-purpose software system for the reduction and analysis of astronomical data, written and supported by the US National Optical Astronomy Observatories (NOAO) in Tucson, Arizona. NOAO is operated by the Association of Universities for Research in Astronomy (AURA), Inc. under cooperative agreement with the National Science Foundation. See iraf.noao.edu for details.

text in Allende Prieto et al. 2014)

- Running mean (CONT=3): the input data are divided by a running mean computed with a window of NCONT pixels.

When continuum normalization is on, the best-fitting models in the output file (`offile`) have been process with the algorithm of choice, while the input data (`ffile`) have not. Since it is usually desirable to compare apples to apples, one can use the keyword SFFILE to specify the name of a new output file that will contain a new version of the input data which has been continuum normalized – the one that has been internally used in FERRE to find the optimal model.

8.7 Multithreading

By default the execution of FERRE is sequential, it analyzes all the targets in the input files in the order given in those files. However, the code implements parallelization over multiple cores in a shared-memory machine using OpenMP. When the keyword NTHREADS is set to a value higher than 1, the list of targets will be split roughly equally among n threads and run in parallel. The output files will have an order different from the input ones while the code is running, but before finishing the execution FERRE will sort them out.

The code performance is usually limited by the speed to access memory (or disk), and therefore the multithreading execution gives only close-to-linear speedups for low values of n, and in general it is not useful to push n beyond a few, and keeping always n smaller than the number of available cores. NTHREADS can be set to 0 for the code to use all the available cores in a processor.

9 Acknowledgements

---

[3]http://www.mhhe.com/engcs/general/chapman/

- *trn.f90*: Truncated Newton Algorithm code written by S. G. Nash (George Mason University). Converted to FORTRAN90 by A. Miller.

- *m_mrgrnk.f90*: Sorting code by M. Olagnon (IFREMER).

- *median.f90*: Median calculation code by A. Miller.

10 Literature using FERRE or FERRE results

The following list is not complete. The main applications of the code so far have been the Century survey galactic halo project, SEGUE, the ELM survey, APOGEE, and the Gaia-ESO survey. Now it is being used in DESI and WEAVE.

1. Rockosi, C. M., Lee, Y. S., Morrison, H. L., et al. 2022, ApJS, 259, 60.

2. Abdurro'uf, Accetta, K., Aerts, C., et al. 2022, ApJS, 259, 35.

3. Phillips, S. G., Schiavon, R. P., Mackereth, J. T., et al. 2022, MNRAS, 510, 3727.

4. García Pérez, A. E., Sánchez-Blázquez, P., Vazdekis, A., et al. 2021, MNRAS, 505, 4496.

5. Horta, D., Mackereth, J. T., Schiavon, R. P., et al. 2021, MNRAS, 500, 5462.

6. Horta, D., Schiavon, R. P., Mackereth, J. T., et al. 2021, MNRAS, 500, 1385.

7. Aguado, D. S., Myeong, G. C., Belokurov, V., et al. 2021, MNRAS, 500, 889.

8. Dalton, G., Trager, S., Abrams, D. C., et al. 2020, Proc. of the SPIE, 11447, 1144714.

9. Jönsson, H., Holtzman, J. A., Allende Prieto, C., et al. 2020, AJ, 160, 120.

10. Price-Jones, N., Bovy, J., Webb, J. J., et al. 2020, MNRAS, 496, 5101.

11. Arentsen, A., Starkenburg, E., Martin, N. F., et al. 2020, MNRAS, 496, 4964.

12. Nidever, D. L., Hasselquist, S., Hayes, C. R., et al. 2020, ApJ, 895, 88.

13. Donor, J., Frinchaboy, P. M., Cunha, K., et al. 2020, AJ, 159, 199.

14. Hayes, C. R., Majewski, S. R., Hasselquist, S., et al. 2020, ApJ, 889, 63.

15. Aguado, D. S., Youakim, K., González Hernández, J. I., et al. 2019, MNRAS, 490, 2241.

16. Garcia-Dias, R., Allende Prieto, C., Sánchez Almeida, J., et al. 2019, A&A, 629, A34.

17. Aguado, D. S., González Hernández, J. I., Allende Prieto, C., et al. 2019, ApJ, 874, L21.

18. Weinberg, D. H., Holtzman, J. A., Hasselquist, S., et al. 2019, ApJ, 874, 102.

19. Souto, D., Allende Prieto, C., Cunha, K., et al. 2019, ApJ, 874, 97.

20. Hasselquist, S., Carlin, J. L., Holtzman, J. A., et al. 2019, ApJ, 872, 58.

21. Mackereth, J. T., Schiavon, R. P., Pfeffer, J., et al. 2019, MNRAS, 482, 3426.

22. Starkenburg, E., Aguado, D. S., Bonifacio, P., et al. 2018, MNRAS, 481, 3838.

23. Anguiano, B., Majewski, S. R., Allende Prieto, C., et al. 2018, A&A, 620, A76.

24. Fu, S. W., Simon, J. D., Shetrone, M., et al. 2018, ApJ, 866, 42.

25. Jönsson, H., Allende Prieto, C., Holtzman, J. A., et al. 2018, AJ, 156, 126.

26. Holtzman, J. A., Hasselquist, S., Shetrone, M., et al. 2018, AJ, 156, 125.

27. Dalton, G., Trager, S., Abrams, D. C., et al. 2018, Proc. of the SPIE, 10702, 107021B.

28. Palicio, P. A., Martinez-Valpuesta, I., Allende Prieto, C., et al. 2018, MNRAS, 478, 1231.

29. Garcia-Dias, R., Allende Prieto, C., Sánchez Almeida, J., et al. 2018, A&A, 612, A98.

30. Abolfathi, B., Aguado, D. S., Aguilar, G., et al. 2018, ApJS, 235, 42.

31. Souto, D., Cunha, K., Smith, V. V., et al. 2018, ApJ, 857, 14.

32. López-Corredoira, M., Allende Prieto, C., Garzón, F., et al. 2018, A&A, 612, L8.

33. Aguado, D. S., Allende Prieto, C., González Hernández, J. I., et al. 2018, ApJ, 854, L34.

34. Badenes, C., Mazzola, C., Thompson, T. A., et al. 2018, ApJ, 854, 147.

35. Wilson, R. F., Teske, J., Majewski, S. R., et al. 2018, AJ, 155, 68.

36. Aguado, D. S., González Hernández, J. I., Allende Prieto, C., et al. 2018, ApJ, 852, L20.

37. García Pérez, A. E., Ness, M., Robin, A. C., et al. 2018, ApJ, 852, 91.

38. Fernández-Alvar, E., Carigi, L., Schuster, W. J., et al. 2018, ApJ, 852, 50.

39. Hayes, C. R., Majewski, S. R., Shetrone, M., et al. 2018, ApJ, 852, 49.

40. Youakim, K., Starkenburg, E., Aguado, D. S., et al. 2017, MNRAS, 472, 2963.

41. Fernández-Trincado, J. G., Zamora, O., García-Hernández, D. A., et al. 2017, ApJ, 846, L2.

42. Majewski, S. R., Schiavon, R. P., Frinchaboy, P. M., et al. 2017, AJ, 154, 94.

43. Aguado, D. S., González Hernández, J. I., Allende Prieto, C., et al. 2017, A&A, 605, A40.

44. Hasselquist, S., Shetrone, M., Smith, V., et al. 2017, ApJ, 845, 162.

45. Blanton, M. R., Bershady, M. A., Abolfathi, B., et al. 2017, AJ, 154, 28.

46. Aguado, D. S., Allende Prieto, C., González Hernández, J. I., et al. 2017, A&A, 604, A9.

47. Linden, S. T., Pryal, M., Hayes, C. R., et al. 2017, ApJ, 842, 49.

48. Recio-Blanco, A., Rojas-Arriagada, A., de Laverny, P., et al. 2017, A&A, 602, L14.

49. Tayar, J., Somers, G., Pinsonneault, M. H., et al. 2017, ApJ, 840, 17.

50. Schiavon, R. P., Johnson, J. A., Frinchaboy, P. M., et al. 2017, MNRAS, 466, 1010.

51. Schultheis, M., Rojas-Arriagada, A., García Pérez, A. E., et al. 2017, A&A, 600, A14.

52. Fernández-Alvar, E., Carigi, L., Allende Prieto, C., et al. 2017, MNRAS, 465, 1586

53. Schiavon, R. P., Zamora, O., Carrera, R., et al. 2017, MNRAS, 465, 501

54. Anders, F., Chiappini, C., Rodrigues, T. S., et al. 2017, A&A, 597, A30

55. del Burgo, C., & Allende Prieto, C. 2016, MNRAS, 463, 1400

56. Allende Prieto, C. 2016, A&A, 595, A129

57. Dafonte, C., Fustes, D., Manteiga, M., et al. 2016, A&A, 594, A68

58. Cunha, K., Frinchaboy, P. M., Souto, D., et al. 2016, AN, 337, 922

59. Fernández-Alvar, E., Allende Prieto, C., Beers, T. C., et al. 2016, A&A, 593, A28

60. Aguado, D. S., Allende Prieto, C., González Hernández, J. I., et al. 2016, A&A, 593, A10

61. Martell, S. L., Shetrone, M. D., Lucatello, S., et al. 2016, ApJ, 825, 146

62. García Pérez, A. E., Allende Prieto, C., Holtzman, J. A., et al. 2016, AJ, 151, 144

63. Bertran de Lis, S., Allende Prieto, C., Majewski, S. R., et al. 2016, A&A, 590, A74

64. Beck, P. G., Allende Prieto, C., Van Reeth, T., et al. 2016, A&A, 589, A27

65. Troup, N. W., Nidever, D. L., De Lee, N., et al. 2016, AJ, 151, 85

66. Brown, W. R., Gianninas, A., Kilic, M., Kenyon, S. J., & Allende Prieto, C. 2016, ApJ, 818, 155

67. Allende Prieto, C., & del Burgo, C. 2016, MNRAS, 455, 3864

68. Recio-Blanco, A., de Laverny, P., Allende Prieto, C., et al. 2016, A&A, 585, A93

69. Schultheis, M., Cunha, K., Zasowski, G., et al. 2015, A&A, 584, A45

70. Holtzman, J. A., Shetrone, M., Johnson, J. A., et al. 2015, AJ, 150, 148

71. Spina, L., Palla, F., Randich, S., et al. 2015, A&A, 582, L6

72. Hayden, M. R., Bovy, J., Holtzman, J. A., et al. 2015, ApJ, 808, 132

73. Alam, S., Albareti, F. D., Allende Prieto, C., et al. 2015, ApJS, 219, 12

74. Tayar, J., Ceillier, T., García-Hernández, D. A., et al. 2015, ApJ, 807, 82

75. Allende Prieto, C., Fernández-Alvar, E., Aguado, D. S., et al. 2015, A&A, 579, A98

76. Fernández-Alvar, E., Allende Prieto, C., Schlesinger, K. J., et al. 2015, A&A, 577, A81

77. Chiappini, C., Anders, F., Rodrigues, T. S., et al. 2015, A&A, 576, L12

78. Carlberg, J. K., Smith, V. V., Cunha, K., et al. 2015, ApJ, 802, 7

79. Lind, K., Koposov, S. E., Battistini, C., et al. 2015, A&A, 575, L12

80. Howes, L. M., Asplund, M., Casey, A. R., et al. 2014, MNRAS, 445, 4241

81. Pinsonneault, M. H., Elsworth, Y., Epstein, C., et al. 2014, ApJS, 215, 19

82. Mikolaitis, Š., Hill, V., Recio-Blanco, A., et al. 2014, A&A, 572, AA33

83. Nidever, D. L., Bovy, J., Bird, J. C., et al. 2014, ApJ, 796, 38

84. Kilic, M., Brown, W. R., Gianninas, A., et al. 2014, MNRAS, 444, L1

85. Smiljanic, R., Korn, A. J., Bergemann, M., et al. 2014, A&A, 570, AA122

86. Bovy, J., Nidever, D. L., Rix, H.-W., et al. 2014, ApJ, 790, 127

87. Allende Prieto, C., Fernández-Alvar, E., Schlesinger, K. J., et al. 2014, A&A, 568, AA7

88. Schultheis, M., Zasowski, G., Allende Prieto, C., et al. 2014, AJ, 148, 24

89. Recio-Blanco, A., de Laverny, P., Kordopatis, G., et al. 2014, A&A, 567, AA5

90. Hayden, M. R., Holtzman, J. A., Bovy, J., et al. 2014, AJ, 147, 116

91. Bergemann, M., Ruchti, G. R., Serenelli, A., et al. 2014, A&A, 565, AA89

92. Ahn, C. P., Alexandroff, R., Allende Prieto, C., et al. 2014, ApJS, 211, 17

93. Xue, X.-X., Ma, Z., Rix, H.-W., et al. 2014, ApJ, 784, 170

94. Anders, F., Chiappini, C., Santiago, B. X., et al. 2014, A&A, 564, AA115

95. Palladino, L. E., Schlesinger, K. J., Holley-Bockelmann, K., et al. 2014, ApJ, 780, 7

96. Majewski, S. R., Hasselquist, S., Łokas, E. L., et al. 2013, ApJ, 777, LL13

97. Frinchaboy, P. M., Thompson, B., Jackson, K. M., et al. 2013, ApJ, 777, LL1

98. Mészáros, S., Holtzman, J., García Pérez, A. E., et al. 2013, AJ, 146, 133

99. Brown, W. R., Kilic, M., Allende Prieto, C., Gianninas, A., & Kenyon, S. J. 2013, ApJ, 769, 66

100. Mészáros, S., & Allende Prieto, C. 2013, MNRAS, 430, 3285

101. García Pérez, A. E., Cunha, K., Shetrone, M., et al. 2013, ApJ, 767, LL9

102. Smith, V. V., Cunha, K., Shetrone, M. D., et al. 2013, ApJ, 765, 16

103. Ahn, C. P., Alexandroff, R., Allende Prieto, C., et al. 2012, ApJS, 203, 21

104. Hermes, J. J., Kilic, M., Brown, W. R., et al. 2012, ApJ, 757, L21

105. Kilic, M., Brown, W. R., Allende Prieto, C., et al. 2012, ApJ, 751, 141

106. Schlaufman, K. C., Rockosi, C. M., Lee, Y. S., et al. 2012, ApJ, 749, 77

107. Brown, W. R., Kilic, M., Allende Prieto, C., & Kenyon, S. J. 2012, ApJ, 744, 142

108. Kilic, M., Brown, W. R., Hermes, J. J., et al. 2011, MNRAS, 418, L157

109. Brown, W. R., Kilic, M., Hermes, J. J., et al. 2011, ApJ, 737, LL23

110. Schlaufman, K. C., Rockosi, C. M., Lee, Y. S., Beers, T. C., & Allende Prieto, C. 2011, ApJ, 734, 49

111. Kilic, M., Brown, W. R., Kenyon, S. J., et al. 2011, MNRAS, 413, L101

112. Aihara, H., Allende Prieto, C., An, D., et al. 2011, ApJS, 193, 29

113. Lee, Y. S., Beers, T. C., Allende Prieto, C., et al. 2011, AJ, 141, 90

114. Brown, W. R., Kilic, M., Allende Prieto, C., & Kenyon, S. J. 2011, MNRAS, 411, L31

115. Allende Prieto, C. 2011, MNRAS, 411, 807

116. Kilic, M., Brown, W. R., Allende Prieto, C., et al. 2011, ApJ, 727, 3

117. Brown, W. R., Kilic, M., Allende Prieto, C., & Kenyon, S. J. 2010, ApJ, 723, 1072

118. Kilic, M., Allende Prieto, C., Brown, W. R., et al. 2010, ApJ, 721, L158

119. Kilic, M., Brown, W. R., Allende Prieto, C., Kenyon, S. J., & Panei, J. A. 2010, ApJ, 716, 122

120. del Burgo, C., Allende Prieto, C., & Peacocke, T. 2010, Journal of Instrumentation, 5, 1006

121. Schlaufman, K. C., Rockosi, C. M., Allende Prieto, C., et al. 2009, ApJ, 703, 2177

122. Allende Prieto, C., Hubeny, I., & Smith, J. A. 2009, MNRAS, 396, 759

123. Abazajian, K. N., Adelman-McCarthy, J. K., Agüeros, M. A., et al. 2009, ApJS, 182, 543

124. Kilic, M., Brown, W. R., Allende Prieto, C., et al. 2009, ApJ, 695, L92

125. Allende Prieto, C., Sivarani, T., Beers, T. C., et al. 2008, AJ, 136, 2070

126. Lee, Y. S., Beers, T. C., Sivarani, T., et al. 2008, AJ, 136, 2050

127. Lee, Y. S., Beers, T. C., Sivarani, T., et al. 2008, AJ, 136, 2022

128. Adelman-McCarthy, J. K., Agüeros, M. A., Allam, S. S., et al. 2008, ApJS, 175, 297

129. Brown, W. R., Beers, T. C., Wilhelm, R., et al. 2008, AJ, 135, 564

130. Kilic, M., Brown, W. R., Allende Prieto, C., Pinsonneault, M. H., & Kenyon, S. J. 2007, ApJ, 664, 1088

131. Dall, T. H., Foellmi, C., Pritchard, J., et al. 2007, A&A, 470, 1201

132. Kilic, M., Allende Prieto, C., Brown, W. R., & Koester, D. 2007, ApJ, 660, 1451

133. Allende Prieto, C., Beers, T. C., Wilhelm, R., et al. 2006, ApJ, 636, 804

134. Brown, W. R., Geller, M. J., Kenyon, S. J., et al. 2005, AJ, 130, 1097

135. Allende Prieto, C. 2004, Astronomische Nachrichten, 325, 604

136. Allende Prieto, C., Beers, T. C., Li, Y., et al. 2004, "Origin and Evolution of the Elements", from the Carnegie Observatories Centennial Symposia. Carnegie Observatories Astrophysics Series. Edited by A. McWilliam and M. Rauch, 2004. Pasadena: Carnegie Observatories

137. Brown, W. R., Allende Prieto, C., Beers, T. C., et al. 2003, AJ, 126, 1362

11   References

- Allende Prieto, C., Fernández-Alvar, E., Schlesinger, K. J., et al. 2014, A&A, 568, A7

- Nelder, J A. & Mead, R. 1965. "A simplex method for function minimization". Computer Journal 7: 308, 313

- Boender, C.G.E., Rinnooy Kan, A.H.G., Strougie, L. & Timmer, G. T. 1982. "A stochastic method for global optimization". Mathematical Programming 22: 125, 140

- Mészáros, S., & Allende Prieto, C. 2013, "On the interpolation of model atmospheres and high-resolution synthetic stellar spectra", MNRAS, 430, 3285

- Powell, M. J. D. 2000, "UOBYQA: unconstrained optimization by quadratic approximation" Report DAMTP 2000/NA14, University of Cambridge

- Dembo, R.S. & Steihaug, T., 1983, "Truncated-Newton Algorithms for Large-Scale Unconstrained Optimization", Math. Prog. 26, 190-212